A DOUBLY-FED INDUCTION GENERATOR DRIVE FOR A WIND ENERGY CONVERSION SYSTEM

P. S. Barendse* and P. Pillay**

** University of Cape Town, Dept. of Electrical Engineering, Private Bag, Rondebosch, 7701, South Africa*
*** Clarkson University, Dept. of Electrical and Computer Engineering, Potsdam, NY 13699, USA*

Abstract: In recent years, there's been a renewed interest in renewable energy sources due to the associated environmental problems and eventual shortage of fossil fuels. Wind energy has gained the most interest of all the renewable energy sources due to the progress in wind related technology [1, 2]. The ability of the doubly-fed induction generator (DFIG) to achieve variable speed control with the reduced cost of converter requirements proves to be extremely attractive for the purpose of wind generation [3]. The reduction in cost is achieved through the control of the torque-speed characteristics of the DFIG from the rotor-side. While this system is commercialized, the companies have not published details of the control strategies. This paper provides the necessary background and results to fill the void between the commercial product produced by a company like Vesta's, and the literature. The hardware setup, simulated results and experimental results are also presented.

Key words: Wind energy conversion systems, Doubly-fed induction generator.

1. NOMENCLATURE

v_a, v_b, v_c	- 3-phase supply voltage (output of variac)
i_a, i_b, i_c	- 3-phase supply-side converter input currents
v_D, v_Q, v_α, v_β	- 2-axis supply voltage
i_D, i_Q, i_α, i_β	- 2-axis supply-side converter input currents
T	- Torque
E	- DC-Link Voltage
s	- slip
L, R	- inductance and resistance of supply-side converter
θ_s, θ_r, θ_e	- stator flux, rotor, supply voltage vector position
θ_r	- rotor position
ω_r	- rotor speed
C	- DC-Link Capacitance
L_s, L_m, L_r	- machine inductances
R_s, R_r	- machine resistances
P	- pole pairs
λ	- flux

Suffices, Superscripts

s, r	- stator, rotor
D,Q	- D-Q axis
α, β	-α-β axis
*	- reference value

2. INTRODUCTION

Due to the economical and environmental benefits, Wind Energy Conversion Systems (WECS) have received tremendous growth in the past decade. The increased interest in wind energy has made it necessary to model and experimentally evaluate entire WECS, so as to attain a better understanding and to assess the performance of various systems. This paper describes a control strategy for a doubly-fed induction generator (DFIG) drive that is in commercial production, but whose technical details have not been published by the manufacturers.

3. FUNDAMENTALS OF WIND POWER

Wind turbine power depends on both the rotor speed and wind speed. The captured power is given by the following equation [4

$$P = \frac{1}{2}\rho C_p A V^3 \tag{1}$$

where ρ mass density of air
A area swept by rotor blades
V wind speed
C_p non-dimensional power coefficient

The relationship between rotor speed and wind speed can be given by

$$\lambda = \frac{\omega_r R}{V} \tag{2}$$

where R wind turbine rotor radius
λ tip speed ratio
ω_r rotor speed

The non-dimensional power coefficient Cp is a function of the tip-speed ratio λ [4]. Fig. 1 illustrates a typical Cp versus λ curve. It is evident from Fig. 1 that for maximum energy capture, the maximum power coefficient and, thus, the optimum tip-speed ratio should be maintained at all wind speeds. The need to vary the rotor speed in accordance to the wind speed for maximum energy capture, establishes the foundation for the preferred choice of Variable Speed WECS.

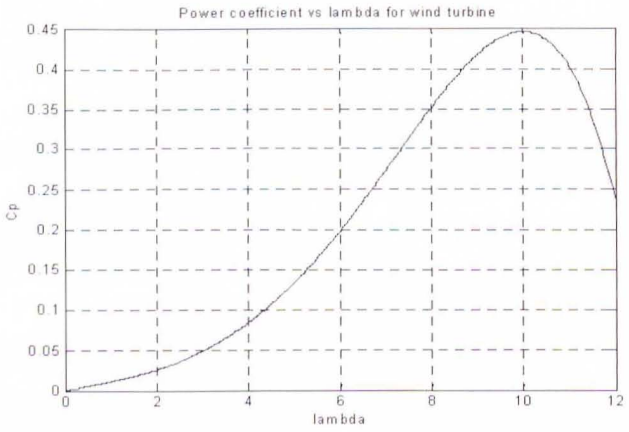

Fig. 1. Power coefficient versus tip speed ratio

4. VARIABLE SPEED DOUBLY-FED INDUCTION GENERATOR FOR A WECS

There are essentially two types of WECS – Constant Speed WECS and the Variable Speed WECS. With Constant Speed WECS, the generator is directly connected to the electrical grid. As a result the speed of the wind turbine is determined by the grid frequency and varies based only on slip [5]. With Variable Speed WECS, the wind turbine rotational speed is allowed to vary so as to extract maximum energy from the wind turbine [6].

For variable speed generation, the wound rotor induction generator proves to be extremely attractive since the converters are located in the rotor circuit, thus reducing the rating and cost of the converter requirements since they need only handle the rotor power [7]. When both the stator and rotor are responsible for the transfer of power in an induction generator they are known as doubly-fed induction generators (DFIG). Fig. 2 illustrates a layout of a Variable Speed DFIG WECS with back-to-back converters in the rotor circuit.

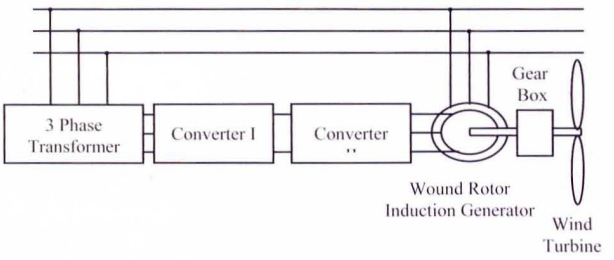

Fig. 2. Variable speed WECS using a DFIG

5. DESCRIPTION OF THE OVERALL SYSTEM

As shown in Fig. 2, the DFIG system uses an AC-AC converter in the rotor circuit. Fig. 3 represents a schematic of the vector control strategy used for the DFIG system. Field orientated control (FOC) of the machine is achieved via the rotor-side converter, which allows for independent control of torque and rotor excitation. The supply-side converter is responsible for maintaining a constant DC-link voltage and control of the power factor. A DC drive is used to emulate the wind turbine [6].

The system operates in two regions;
(1) Sub-synchronous region: the rotor speed lies below synchronous speed, and the rotor absorbs power from the grid.
(2) Super-synchronous region: the rotor speed lies above synchronous speed, and the rotor delivers power to the grid.
The amount of power absorbed and delivered by the rotor is slip dependant [8].

5.1. Control of the Supply-Side Converter

The supply-side converter is used to maintain a constant DC-link voltage, regardless of the direction of rotor power flow. A vector control approach is used, as shown in Fig. 4, whereby independent control of active and reactive power is achieved.

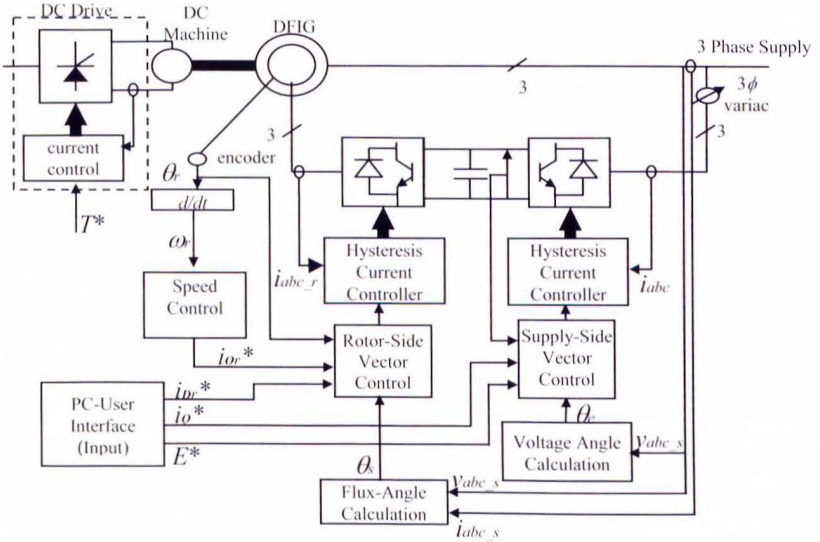

Fig. 3. Schematic of a vector control system for a doubly-fed induction generator using back-to back converters

The supply voltage angular position is calculated as

$$\theta_e = \arctan\left[\frac{V_\beta}{V_\alpha}\right] \tag{3}$$

where θe represents the supply voltage vector position [7].

The DC-link voltage can be controlled via i_D. The control scheme thus derives the i_D demand from the DC-link voltage error through a PI controller. The i_Q demand is responsible for the transfer of reactive power. Once the setpoint 3-phase currents have been determined, they are processed by a hysteresis current controller, which determines the switching pattern of the IGBT converter.

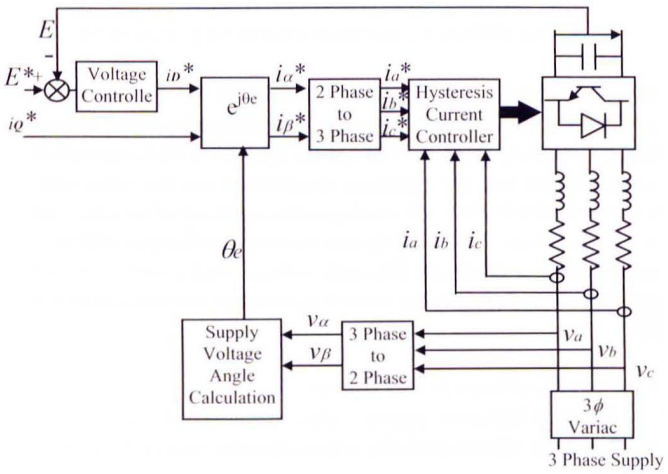

Fig. 4. Schematic of vector control for the supply-side converter

5.2. *Control of the Rotor-Side Converter*

Field orientated control from the rotor-side is achieved in the synchronously rotating DQ reference frame. The D-axis is aligned with the stator-flux vector position, which sets the Q-axis stator-flux component to zero. In this way, a decoupled control between the electrical torque and the magnetic field is obtained [7].

Since

$$\lambda_{QS} = 0 \tag{4}$$

the torque is described as follows

$$T = -\frac{P}{3}\frac{L_m}{L_s}\lambda_{DS} i_{Qr} \tag{5}$$

Fig. 5 illustrates the schematic block diagram for the machine control. i_{Dr}* is used to control the rotor excitation, however assuming that the reactive power to the machine is supplied by the stator, i_{Dr}* may be set to zero [7]. The torque is proportional to $\lambda_D i_{Qr}$, thus once T* is determined via the speed controller, i_{Qr}* is calculated (using the above torque equation). The 3-phase current setpoints are then achieved using the correct transformations, and the desired currents into the machine are attained via the use of the hysteresis current controller.

The stator flux is determined as follows

$$\lambda_{\alpha S} = \int (V_{\alpha S} - R_S i_{\alpha S})dt \tag{6}$$

$$\lambda_{\beta S} = \int (V_{\beta S} - R_S i_{\beta S})dt \tag{7}$$

The stator flux angle is calculated as follows

$$\theta_s = \arctan\left[\frac{\lambda_{\beta S}}{\lambda_{\alpha S}}\right] \tag{8}$$

where θs represents the stator flux position [7]. The ω_r error is processed by a PI controller to give the setpoint torque (T*). The diagram below indicates the complete vector control for the rotor-side converter using the above formula's to calculate the stator flux and stator flux angle.

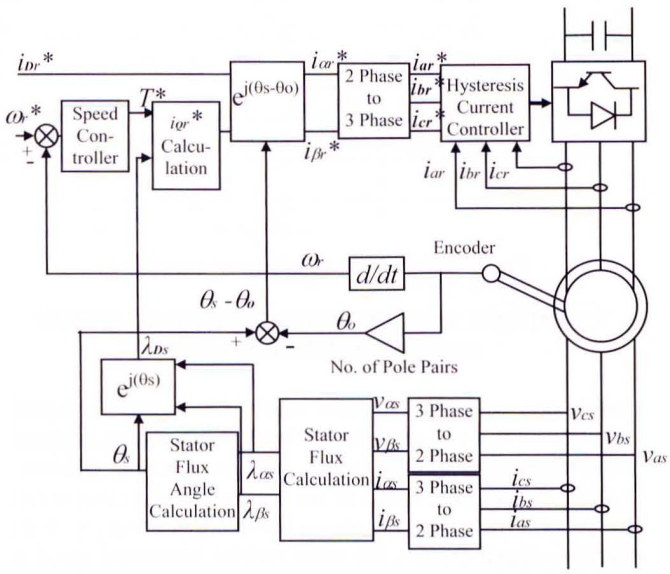

Fig. 5. Schematic of vector control for the rotor-side converter

6. EXPERIMENTAL SETUP

Fig. 6 shows a picture of the overall experimental system. The wound rotor induction machine (WRIM) used is a 2.2kW, 3-Ph, 380V, 50Hz, 4 pole machine, whose parameters are given in the Appendix. Two hysteresis current controlled converters are placed in the rotor circuit, which provides the supply- and rotor-side control. Extra resistors and chokes are added to the supply-side converter, which are located between the 3 phase variac and the supply-side converter. The extra resistors and inductors added onto the supply-side converter is, R =0.1Ω and L=20mH. The DC-link voltage is maintained at 300V and the supply-side 3-phase voltage is set to 100V (i.e output of the variac). The DC drive used to emulate the wind turbine consists of a 2.2kW DC machine, which is torque controlled by an AC-DC thyristor converter.

A DS 1104 R&D Controller Card is used to perform the computational and control tasks for both converters. Some of the more important features of the card include the main processor, which is a MPC 8420, PowerPC 603e core with a 250MHz clock frequency. It also consists of 8 ADC channels, 20-bit digital I/O ports and a slave DSP subsystem from Texas instruments (i.e. DSP TMS 320F240).

The controller card forms part of the Advanced Control

Educational Kit and is fully programmable from the Matlab-Simulink block diagram environment, provided that the real-time interface software, supplied by dDSPACE, is installed. This software translates the simulink model into equivalent C-code for processing by the board. Although this doesn't prove to be the most efficient means of control, it does allow for rapid testing of control prototypes. The card may also be programmed directly from C-code, making the card as efficient as any other processor. The ACE Kit also consists of an experimental software package (ControlDesk) which allows for real-time control of the system. The kit essentially upgrades a PC into a development system for rapid control prototyping.

The converters used are standard 100A commercial IGBT inverters. The inverters are switched at a maximum frequency of 5kHz during the simulated and experimental tests, due to the computational ability of the controller card. However, this switching frequency employed in the prototype confirms that the control techniques can be extended to higher power levels.

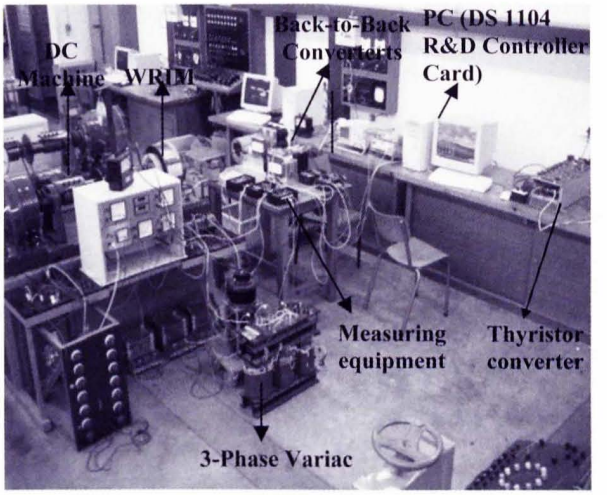

Fig. 6. Experimental setup in the laboratory

7. SIMULATION RESULTS

7.1. Supply-side converter

The DC-link voltage is maintained at 300V while the converter is connected to a 100V supply. The diagrams below indicate the ability of the supply-side converter to allow for bidirectional power flow. Figs 7 and 8 indicate the supply voltages and currents for one of the phases. These results were attained, with i_Q* set to zero. Fig. 7 shows a phase displacement of 0° between the phase voltages and phase currents for the converter operating in rectifying mode, corresponding to sub-synchronous operation. Fig. 8 shows a phase displacement of 180° between phase voltages and phase currents for the converter operating in inverting mode, corresponding to super-synchronous operation.

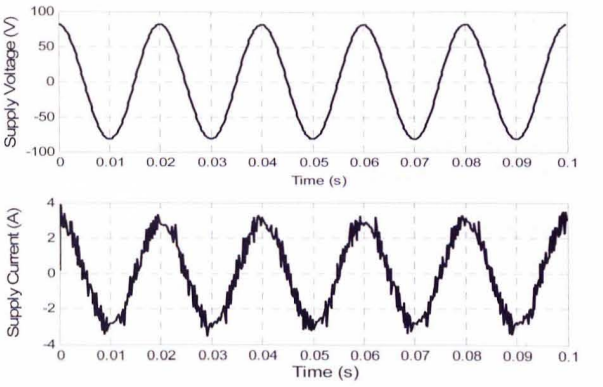

Fig. 7. Simulation results for the supply-side converter during rectifying mode

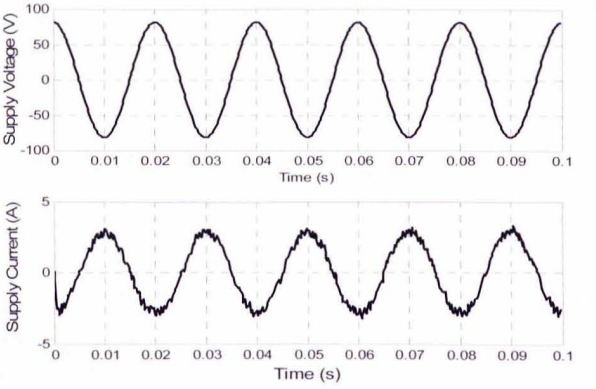

Fig. 8. Simulation results for the supply-side converter during inverting mode

Fig. 9 shows the dynamic response of the DC-Link voltage as the speed of the generator is ramped up. A fairly slow PI controller is used for the supply-side converter since the response speed of the DC-link voltage is not critical. The overshoot does not surpass 305V for the fastest change in speed.

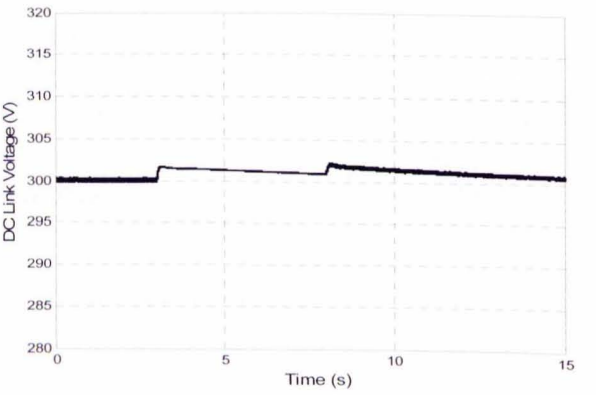

Fig. 9. Simulated DC-Link voltage for operation through synchronous speed

7.2. Rotor-side converter

The simulation results indicate the generator operating at speeds 25% below (1120rpm) and 25% above (1880rpm) the synchronous speed at a constant Torque of 7Nm. Fig. 10 shows a speed profile of the DFIG as it is ramped up in speed from 1120rpm to 1880rpm over 5 seconds, through the synchronous speed. Fig. 11 shows the rotor phase currents when passing through the synchronous speed.

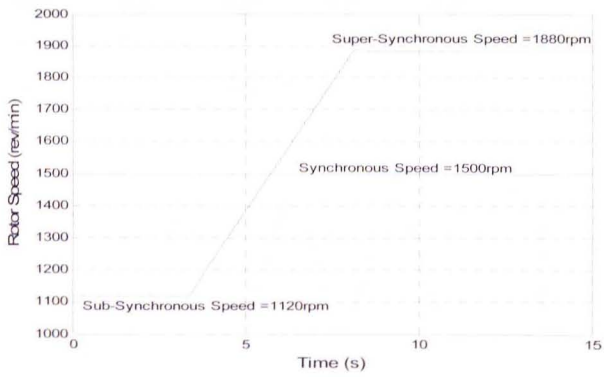

Fig. 10. Rotor speed response for operation through synchronous speed

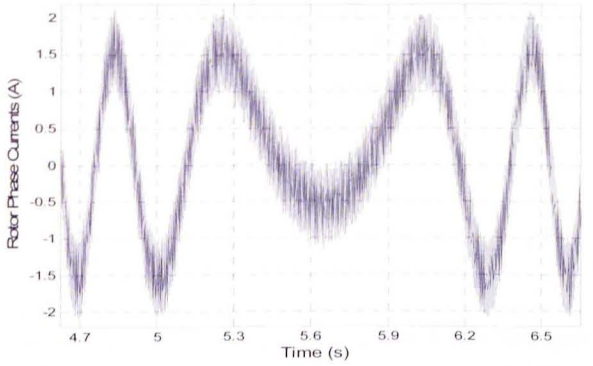

Fig. 11. Rotor phase current response for operation through synchronous speed

Figs 12 and 13 illustrate the bi-directional power flow capabilities of the rotor during sub-synchronous and super-synchronous operation. If the stator generates 1p.u. at a slip s, the power delivered by the rotor is –s p.u. (neglecting losses).

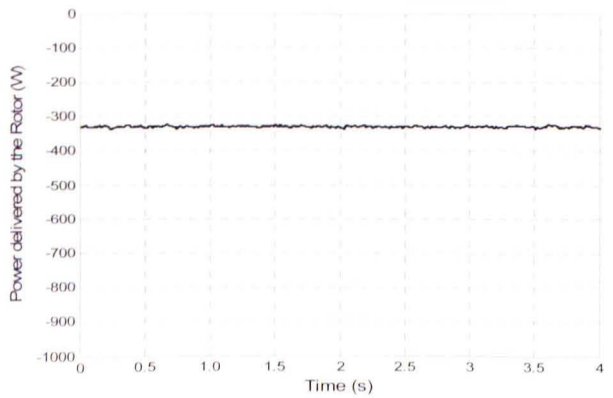

Fig. 12. Power delivered by the rotor during sub-synchronous operation

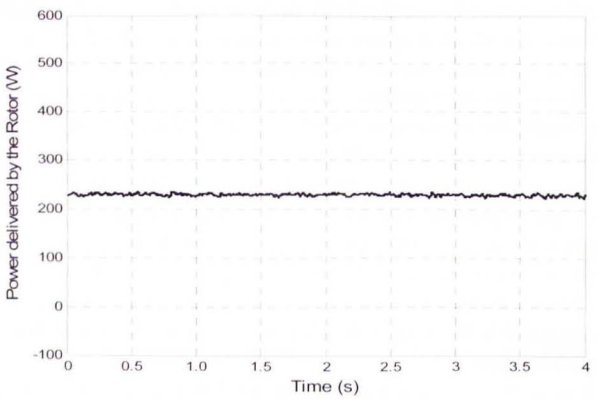

Fig. 13. Power delivered by the rotor during super-synchronous operation

8. EXPERIMENTAL RESULTS

8.1. Supply-side converter

The experimental results shown below were attained from similar conditions and tests as that of the simulations. The DC-Link voltage is maintained at 300V, while the variac is kept at 100V. Figs 14 and 15 show the supply voltages and currents for a single phase, during sub- and super-synchronous generation. The 0° and 180° phase displacement between the phase voltages and currents for the two respective modes are again evident, as with the simulations.

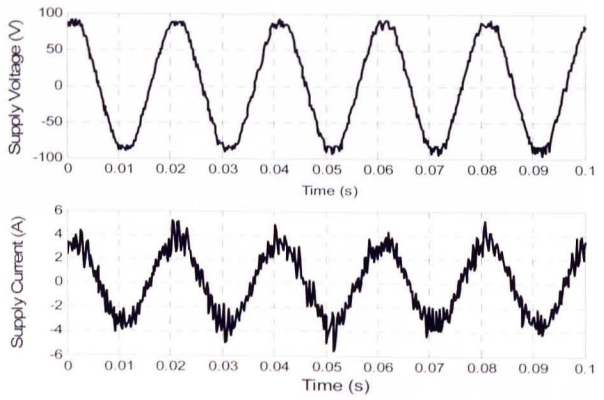

Fig. 14. Experimental results for the supply-side converter during rectifying mode

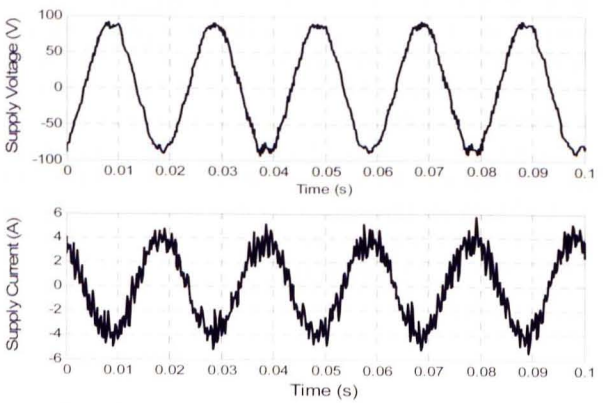

Fig. 15. Experimental results for the supply-side converter during inverting mode

Fig. 16 shows the dynamic response of the experimental DC-Link voltage for a ramp up in generator speed. The use of the slow PI controller is evident by the slow response of the voltage to track the setpoint voltage of 300V.

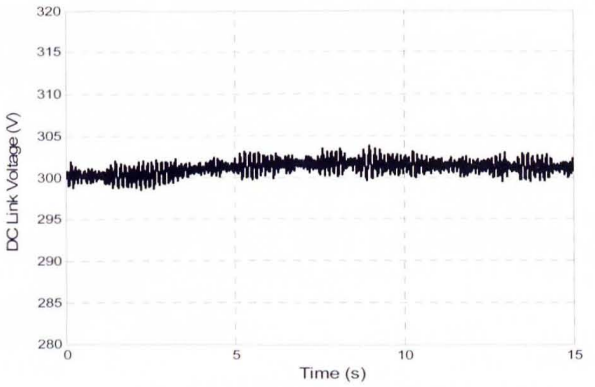

Fig. 16. Experimental DC-Link voltage for operation through synchronous speed

8.2. Rotor-side converter

Numerous tests were performed in both steady state and transient conditions, to test the performance of the rotor-side converter. The results shown below show the generator operating at 25% below (1120rpm) and 25% above (1880rpm) the synchronous speed, at a constant torque of 7Nm. This is identical to the conditions under which the simulations were performed.

Fig. 17 shows the speed response of the generator as the speed is ramped up from 1120rpm (sub-synchronous speed) to 1880rpm (super-synchronous speed) over 5s. The system requires approximately 4 seconds for the generator to stabilise at 1880rpm, unlike the immediate clamping of the simulated results. This is contributed to certain non-ideal conditions, which the simulations do not take into account. Fig. 18 displays the rotor phase currents as the generator passes through synchronous speed.

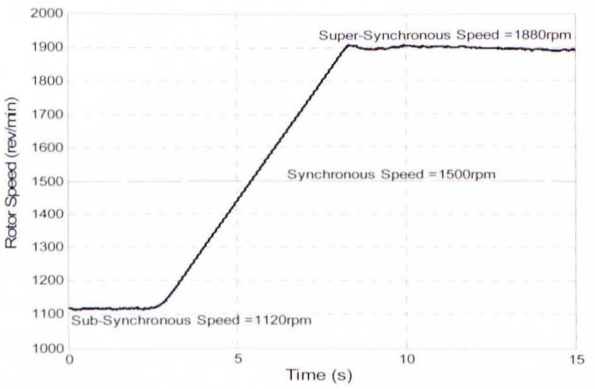

Fig. 17. Rotor speed response for operation through synchronous speed

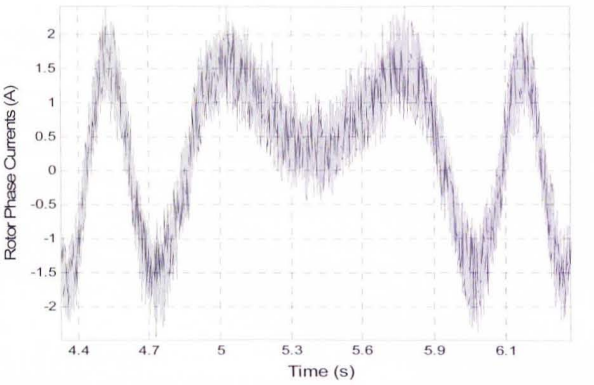

Fig. 18. Rotor phase current response for operation through synchronous speed

Figs 19 and 20 show the power delivered by the rotor during sub- and super-synchronous operation. The bi-directional capabilities of the system is once again evident, however the losses are greater than predicted by the simulations.

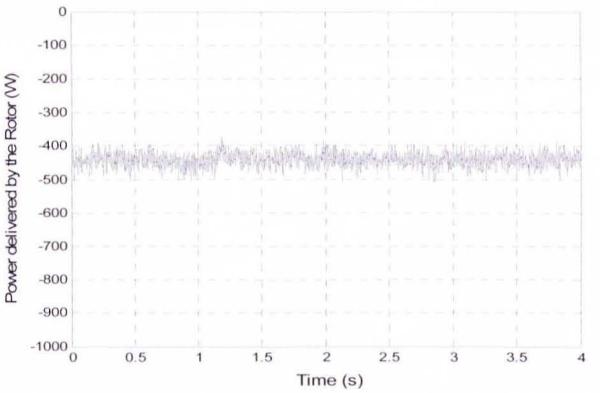

Fig. 19. Power delivered by the rotor sub-synchronous operation

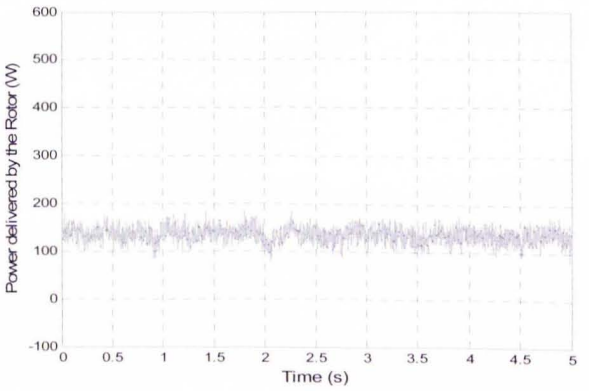

Fig. 20. Power delivered by the rotor during super-synchronous operation

9. CONCLUSIONS

The paper has described the vector control strategy for a doubly-fed wind energy drive, with vector control from the rotor-side. The results attained for the system have been shown and discussed. They show the system operating under various steady state and transient conditions. The DFIG system was simulated so as to validate the control strategies and operation of the experimental system. The supply-side converter was shown to control the DC-link voltage and the reactive power flow while the rotor-side converter was shown to control the speed of the generator, with the use of a PI controller. The bi-directional power flow capabilities of the drive were also shown as the generator operated within the sub-synchronous and super-synchronous regions. This paper fills the void in the literature by describing mathematically and experimentally verifying a commercial product, thus allowing further research from the community.

10. REFERENCES

[1] C.V. Nayar, J.H. Bundell, "Modelling and Simulation of a Wind-Driven Wound Rotor Induction Generator with Tip-Speed Ratio Control", Electric Energy Conference 1987, Adelaide, 6-9 October 1987

[2] B. Connor, W. E. Leithead, "Performance Assessment of Variable-Speed Wind Turbines", Opportunities and Advances in Internnational Power Generation, 18-20th March 1996, Conference Publication No.419, IEE, 1996

[3] Chris S. Brune, "Experimental Evaluation of Variable Speed, Doubly-Fed Wind-Power Generation System", IEEE Transactions on Industry Applications, Vol.30, No. 3, May/June 1994

[4] S.R. Chellapilla and B. H. Chowdhury, "A Dynamic Model if Induction Generators for Wind Power Studies", IEEE,2003

[5] B. Connor, W. E. Leithead, "Performance Assessment of Variable-Speed Wind Turbines", Opportunities and Advances in Internnational Power Generation, 18-20th March 1996, Conference Publication No.419, IEE, 1996

[6] P.Barendse and P. Pillay, "Matlab Simulation of a Doubly-Fed Induction Generator (DFIG) System in it's Application to Wind Energy Generation", SAUPEC, Jan 2004

[7] R. Pena, J.C. Clare and G.M. Asher, "Doubly Fed Induction Generator using Back-to-Back PWM Converters and its Application to Variable Speed Wind Energy Generation", IEE Proc.-Electr. Power Appl., Vol. 143, No. 3, pp231-241, May 1996

[8] Rajib Datta, V.T. Ranganathon, "Variable Speed Wind Power Generation Using Doubly Fed Wound Rotor Induction Machine-a comparison with alternative schemes," IEEE Transactions On Energy Conversion, Vol.17, No. 3, pp 414-421, September 2002

11. APPENDICES

Wound rotor induction machine ratings:
Rated Power = 2.2kW
Rated Voltage =380V
Rated current = 4A
Speed at rated power = 1375 rpm

Stator connection = wye
Rotor connection = wye
Pole pairs = 2
$R_s = 6.6\Omega$
$R_r = 4.61\Omega$
$L_s = 0.4459H$
$L_r = 0.4459H$
$L_m = 0.4178H$